Damage prediction of turbine start-up sequence of a full size frequency converter variable speed pump-turbine using transient stress signals

J Schmid¹, S Alligné¹, C Nicolet¹, A Gauthier², M Seydoux², E Vagnoni², N Hugo³

- ¹ Power Vision Engineering Sarl, CH-1025 St-Sulpice, Switzerland
- ² Technology Platform for Hydraulic Machines, École Polytechnique Fédérale de Lausanne, Lausanne, Switzerland

E-Mail: jeremy.schmid@powervision-eng.ch

Abstract. Hydropower plants have a high ability to control the stability of the electrical power system, since they are dispatchable energy sources and have a fast response time for providing ancillary services. Therefore, they are key players to guarantee the energy balance of renewable power systems being deployed today. It is well-known that these ancillary services lead to an extended and flexible operation of hydraulic machines, resulting in accelerated degradation of the mechanical components. The number of start-ups and stops is significantly increasing, and, therefore, the assessment and forecast of the damage of a specific start-up sequence is an essential stage to minimize the impact on the lifetime of mechanical components. This paper presents a method for predicting the damage of a start-up sequence by using stresses measurements on the runner blades. Reduced-scale model tests of a Francis-type pump-turbine under transient and steady state conditions have been performed at EPFL Technology Platform for Hydraulic Machines. These experimental measurements include on-board runner strain gauges and pressure fluctuations sensors which are used to build a transient signal map by means of discretized transient signals and predict the runner damage. By using this transient mapping method, the cumulative runner damage can be forecasted while recombining the entire time stress signal of a start-up sequence by taking into account the mean stress value, which is one of the parameters influencing the total damage of the runner. The preliminary results with the proposed method predict a fairly accurate shape of the stress signal in the time domain of a given start-up sequence. Additionally, it predicts the damage runner's order of magnitude by using standard stress-life cumulative damage calculation. This study is part of the European innovation project XFLEX HYDRO, which aims to demonstrate the flexibility of hydropower plants, such as the Z'Mutt 5 MW reversible Francis-type pump-turbine variable speed unit equipped with a Full Size Frequency Converter (FSFC), which is used as case study in the framework presented in this article.

1. Introduction

In order to meet the European Union's decarbonization targets by 2050, the electricity supply system will have to adapt strongly to the dynamics of variable renewable energies [1]. These energy productions are stochastic and non-dispatchable, which implies challenges in terms of managing the stability of the power network. The European XFLEX HYDRO H2020 project aims to demonstrate, using new approaches, the control and flexibility capabilities of hydroelectric power plants and, consequently, their key role in the future electricity supply system [1]. The Z'Mutt pumping station in Zermatt, Switzerland, which is part of the Grande Dixence hydroelectric power plant, feeds the reservoir of Lacs des Dix, has

³ Alpiq SA, Lausanne, Switzerland

been selected as one of the XFLEX Hydro demonstrators. A new 5 MW reversible Francis pump-turbine equipped with a Full Size Frequency Converter (FSFC) allowing for high flexibility during start-up and stop sequence was recently put in operation at Z'Mutt pumping station. The PTMH (Platform Technique Machine Hydraulique, EPFL, Lausanne, Switzerland) carried out measurements on a reduced scale model similar to the Z'Mutt Francis pump-turbine [7], which are being used to implement the proposed method presented in this paper. The operating flexibility of hydroelectric units may result in accelerated degradation of hydromechanical components caused, for example, by increased start and stop sequences, and also switching from pumping mode to turbine mode [3], [4]. The transient start-up sequence of the unit is known to be a critical and constraining operating condition for the mechanical components and can reduce their lifetime [3], [5]. The improvement of start-up trajectories could reduce wear and premature fatigue of the hydraulic runner. Furthermore, the variable speed technology using a full size frequency converter provides more flexibility for start-up sequences, as the rotational speed is no longer driven by the opening of the guide vane but it is a control parameter of the frequency converter during turbine start-up sequence. These optimized start-up trajectories make it possible to avoid speed-no-load unstable operating conditions and high-load regions [6],[7],[8],[12].

The paper introduces an approach for predicting hydraulic runner damage during a start-up sequence. The method involves discretised transient signal mapping using the Voronoi diagram. By analysing the complete time stress signal of the start-up sequence and considering the mean stress value, which is a crucial factor in determining total runner damage, the cumulative runner damage can be anticipated through this transient mapping approach. The effectiveness of the proposed method is demonstrated using experimental data from model tests conducted by the PTMH (Technology Platform for Hydraulic Machines, EPFL) [7].

2. Z'Mutt power plant demonstrator

Z'Mutt is a Pumping Station located in Zermatt, Switzerland. This pumping station is equipped with two 30 MW pump units (U1, U2), two 14 MW pump units (U3, U4) and one 5 MW reversible pump-turbine unit (U5), see Figure 1. The unit U5, which is the scope of the study, is equipped with an asynchronous motor-generator, driven by a FSFC. The Francis pump-turbine is characterized by a specific speed of Nq = 54 and a unit mechanical time constant of tm=1.3 s. The main hydraulic characteristics are given in Figure 1.

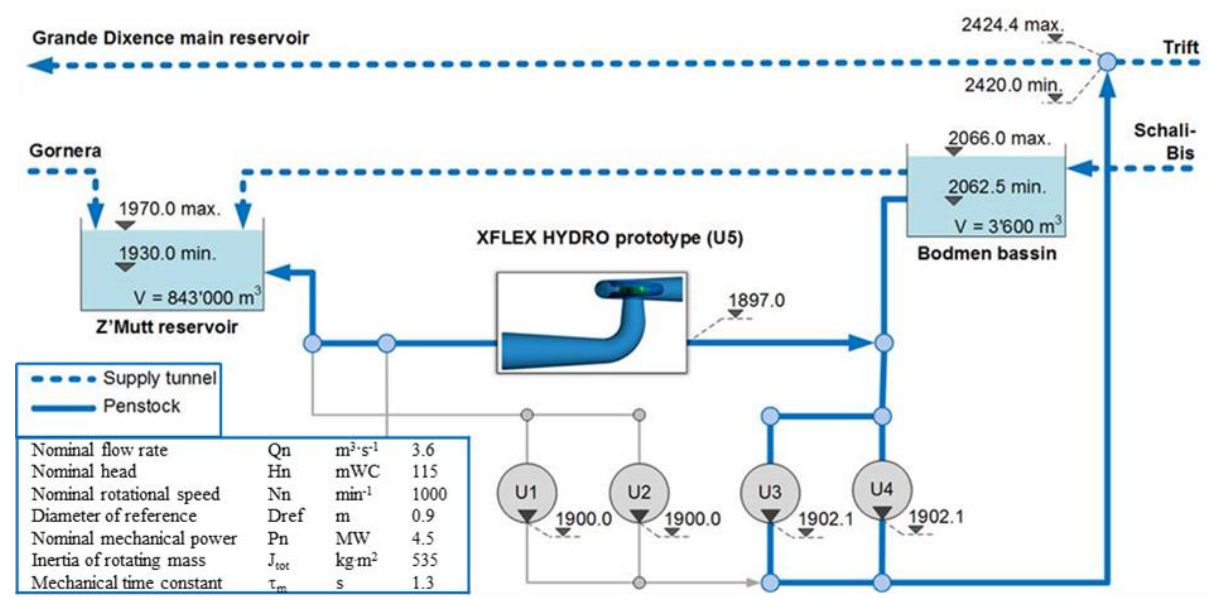


Figure 1: Schematic of the Z'Mutt pumping station.

3. Methodology

3.1. Transient mapping of stress signals using Voronoi diagram

To optimize the start-up trajectory and minimize pump-turbine damage effectively, it is advantageous to create a comprehensive instantaneous damage map that incorporates all runner stress signal information, encompassing both high-cycle fatigue (HCF) and low-cycle fatigue (LCF) values [9]. By utilizing the complete transient stress signal, valuable data on the mean stress value can be retained. The proposed method aims to preserve both HCF and LCF quantities when predicting the stress signal for a new turbine start-up trajectory, by reusing the transient signals themselves to reconstruct a temporal stress signal. The map construction can be combined with several values, such as transient and stationary values, to best map the N11-Q11 frame of the pump-turbine characteristic.

To predict the damage related to a given start-up trajectory of the pump-turbine, the N11-O11 operating range, representing the transient behavior of the start-up, is subdivided into transient stress cells through Voronoi decomposition. The Voronoi diagram can indeed be used, by exploiting its geometric properties, for predicting trajectories in various contexts, especially in motion planning and pathfinding applications [13]. In our case, the aim is to find the best trajectory for a turbine start-up in the N11-Q11 frame, in order to minimize runner damage by optimizing the trajectory between the rest operation and its targeted operating point. The principle is that, given a point in a set of coplanar points, you can draw a boundary around it that includes all points closer to it than to any other point in the set. This boundary defines a single Voronoi polygon. The construction of all Voronoi polygons for each point in the set is called a Voronoi diagram. It is therefore possible to extract runner time stress signal at the nearest operating point in the N11-Q11 frame in order to predict a new trajectory. Each cells of the map hold normalized transient stress signals of a specific time ($\Delta t=2s$), allowing for the prediction of stress distribution in the time domain for a new sequence trajectory in N11(t) and Q11(t), see Figure 2. The signal stored is normalized with the dynamic pressure $C_{\sigma} = \sigma/(1/2 p^* U^2)$ to keep in the information of the absolute rotational speed. Finally it generates a discretized map of a time signal in the N11-Q11 frame.

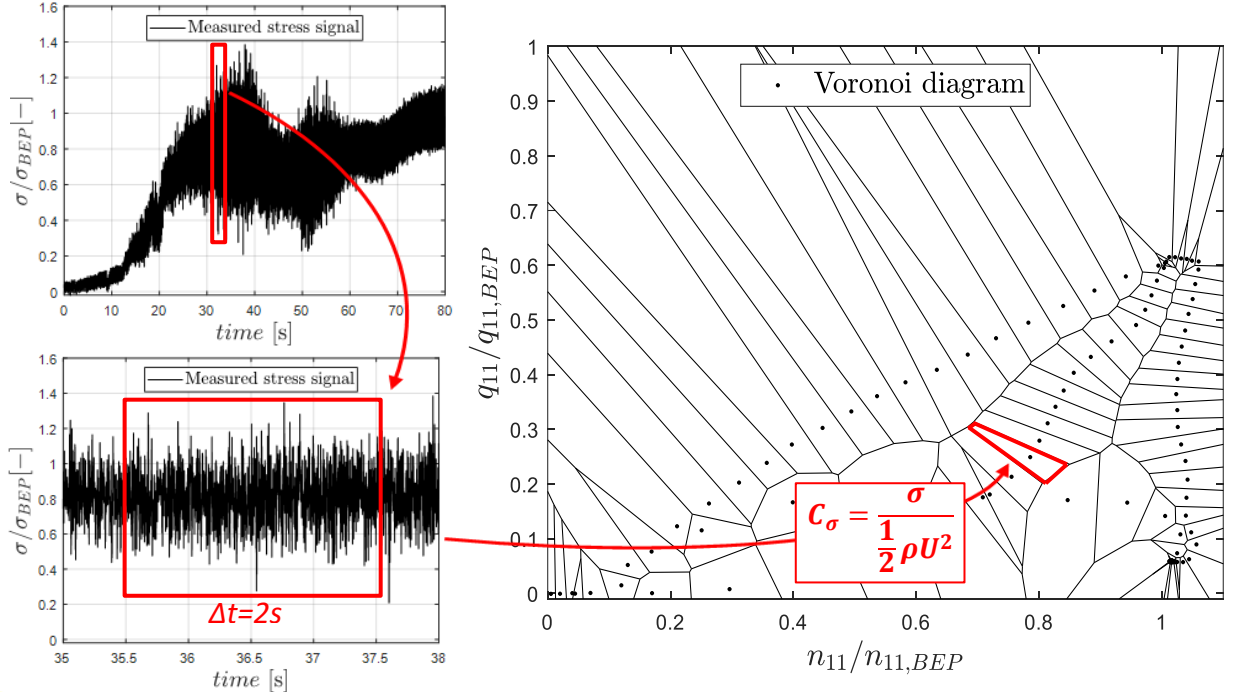


Figure 2: Representation of the creation of the Voronoi diagram with the time-stress signal. **Top-left**: Full time stress signal of a specific start-up trajectory. **Bottom-left:** Discretization of the time signal for each Voronoi cell. **Right**: Voronoi diagram with dynamic pressure normalized for the N11-Q11 pump-turbine operating range normalized by the BEP.

3.2. Cumulative damage calculation

To calculate the number of fatigue cycles in order to obtain the cumulative damage, the method is based on the standard stress-life approach for a given load-time history. Overall, the process involves analyzing the stress load history of a start-up sequence using Rainflow cycle counting algorithm [10], correcting stresses using Goodman's relationship to takes into account both the mean stress and the alternating stress to assess the fatigue damage more accurately. Then calculating cumulative damage using Miner's rule and Wöhler's curve approximated by Basquin's law [11]. Basquin's law is used to approximate the central part of the S-N curve with a power law relationship, which simplifies the calculation. The S-N curve used to compute the cumulated linear damage is extracted from Sonsino et al. (1990). [14]. This makes it possible to assess the fatigue life and runner damage under considerations to be able to compare different turbine start-up trajectories in the order of magnitude. The S-N curve utilized in this paper differs from the one employed in prior research [8]. There are slight variations, attributed to these differing assumptions, in the calculation of cumulative damage between these two investigations.

3.3. Experimental data

In order to assess the damage of a transient operating sequence, rotating frame on-board strain measurement have to be obtained. It requires complex instrumentation that is not commonly added to the runner of a scale prototype because in reality it represents additional cost that the HPP operator wants to avoid. For reduced-scale model tests, it is more feasible to well instrument the runner with on-board strain gauges. In our case, the experimental data are from the reduced-scale model tests of a similar Francis pump-turbine under transient and steady state conditions that have been performed at PTMH. These experimental measurements include on-board runner strain gauges located at the leading edge which are used to build a transient signal map by means of discretised transient signals and predict the runner damage [7]. For more information on the experimental campaign, see [7]. During the measurement campaign, transient start-up sequences were performed. There are four different types of start-up, three associated with variable speed technology (linear var-speed start-up, BEP tracking var-speed start-up and 2-slopes var-speed start-up) and one with classical fixed speed technology passing through speed-no-load condition.

4. Results

4.1. Prediction of stress signal

The four different pump-turbine start-ups used are shown in Figure 3. Among these start-ups, there are three start-ups with variable-speed technology and one with fixed-speed technology. The variable-speed start-ups are as follows: (A) 2-slopes start-up, (B) BEP tracking start-up and (C) linear start-up. The 2-slopes start-up is determined by 2-stages for the guide vane opening (y) and two stages for the rotational speed (n). The BEP tracking start-up is determined by the efficiency hill-chart following the best operating point during the pump-turbine start-up. The linear start-up, a simple linear law is implemented for the guide vane opening (y) and the rotational speed (n), with a delay between guide vane and rotational speed to avoid excessive power consumption at the very beginning of the start-up. And finally, the fixed-speed start-up (D) illustrates a classical start-up passing through the speed-no-load condition before synchronizing the pump-turbine to the power grid. The total duration of the different pump-turbine start-ups vary, between 16s, 22s and 60s to reach the target operating point.

The start-up sequence with variable-speed technology allows greater flexibility and therefore enables faster sequences than with fixed-speed technology. In order to illustrate the method described in this paper, Voronoi diagrams are created on the basis of the stress-signal information from three of the four available start-up transient trajectories, in order to predict the 4th start-up trajectory in the N11-Q11 operating range. This avoids having all the stress information in the Voronoi cells of the trajectory to be

predicted. The method described enables to establish stress-signal of a new trajectory within the N11-Q11 operating range without possessing the precise reference of a specific start-up trajectory and then allows the time stress signal prediction from an unknown start-up to be evaluated.

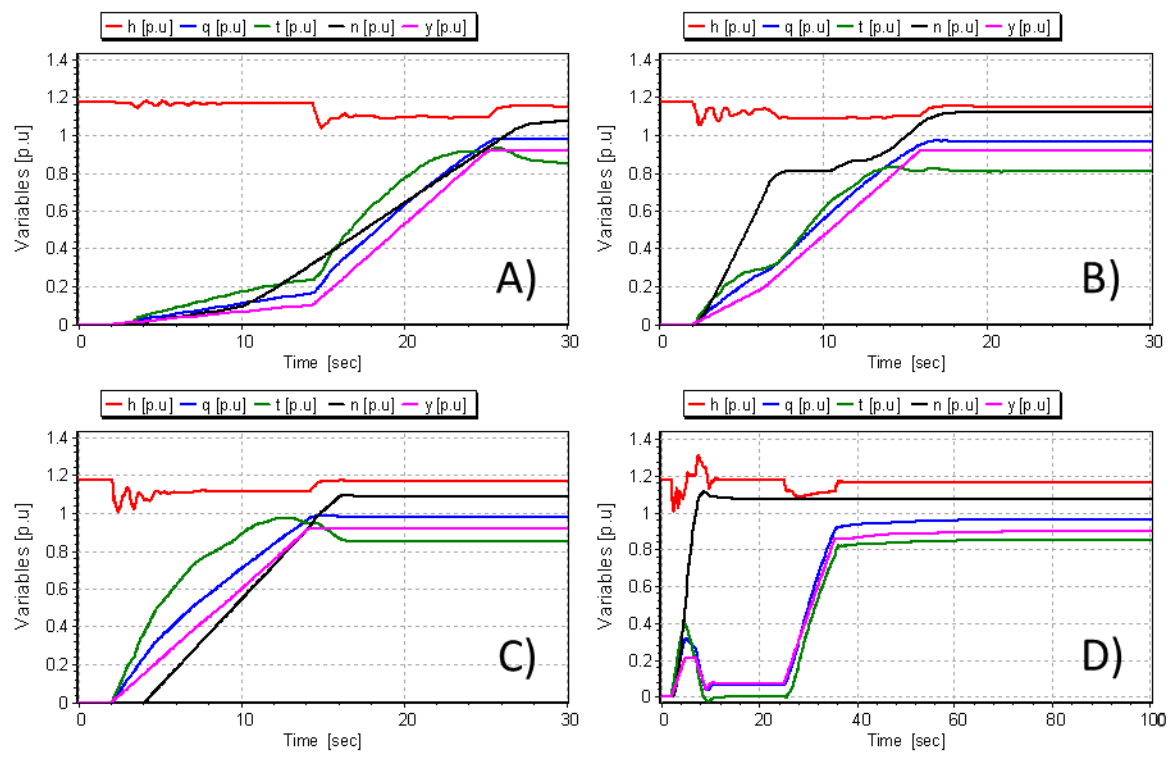


Figure 3: Representation of the transient behaviour of the 4 start-up trajectories in time domain with the head h, discharge q, mechanical torque t, rotational speed n, guide vane opening y. A) 2-slopes start-up trajectory, B) BEP tracking start-up trajectory, C) linear start-up trajectory and D) standard fixed-speed start-up trajectory passing through SNL condition.

The results of the Voronoi diagram are shown in Figure 4. For each of the three different predictions, and thus each diagram is made up of different cells with Δt =2s time discretization. The start-up trajectories in red are superposed to the cells containing the time stress signal information, which can be reconstructed over the full startup by combining the different cells together. Clearly, the predicted trajectory does not pass through the central points of the Voronoi cells, and will therefore be reconstructed using the nearest points.

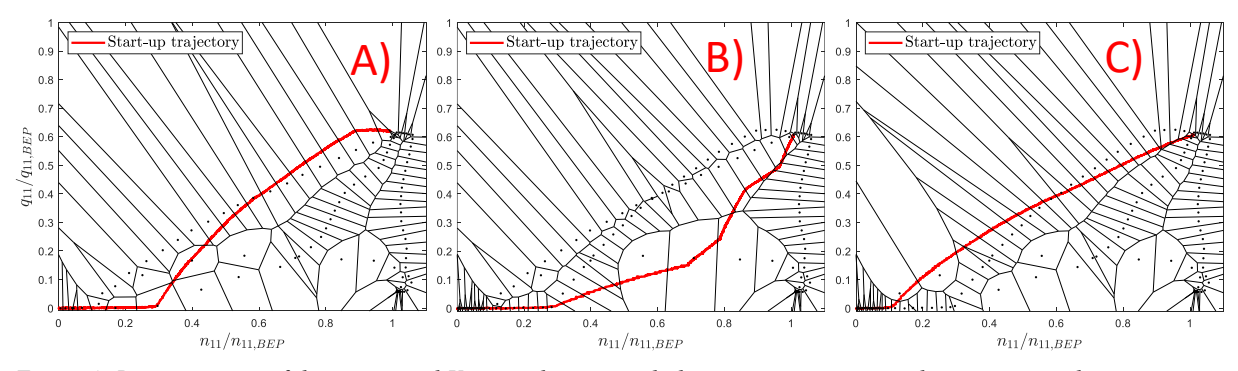


Figure 4: Representation of the superposed Voronoi diagram with the start-up trajectory to be reconstructed in time stress-signal: A) 2-slopes start-up trajectory, B) BEP tracking start-up trajectory. C) linear start-up trajectory.

The three predicted time stress signal (red) for each trajectories are shown in Figure 5 and they are compared with the signals measured on the reduce-scale model (black). The average signals are also represented to allow comparison of the amplitude of the mean stress value over time. The overall predictions are relatively accurate to the measurements in terms of time signal pattern. The most significant deviations are observed at the beginning of the start-up sequence, but the envelopes of stress fluctuations are well reproduced. The linear start-up trajectory (C) is the least well predicted, with the largest deviation. The reason is that this trajectory is the furthest away in the N11-Q11 domain and therefore plays the role of boundary data in the other predictions when the Voronoi diagram are built.

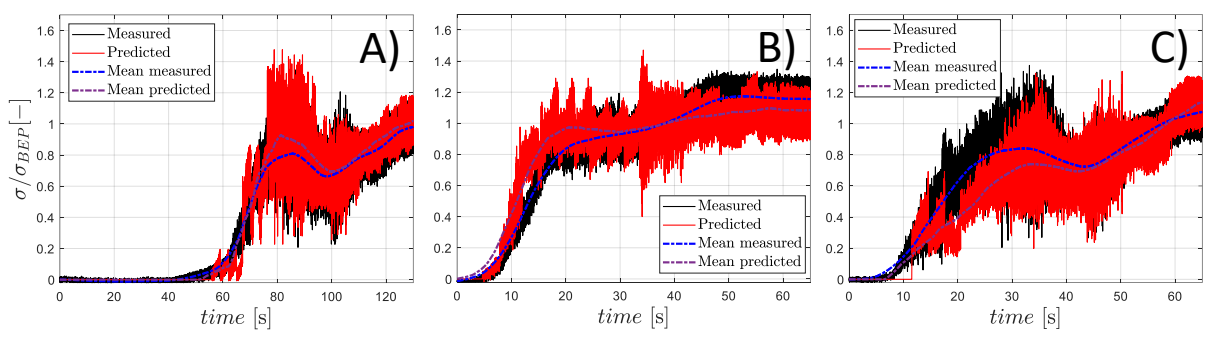


Figure 5: Results of the predicted time stress-signal compared to the measured time stress-signal including also the comparison of the average: A) 2-slopes start-up trajectory, B) BEP tracking start-up trajectory, C) linear start-up trajectory.

4.2. Prediction of cumulative damage calculation

After obtaining and predicting the time-stress signal, the next step involves computing the cumulative damage incurred by the runner. This computation aims to facilitate a comparison between various start-up trajectories with the ultimate goal of optimizing the runner's operational lifespan. The accumulated damage value (D) and the damage distribution (di) obtained from the predicted stress signals are compared to the stress signals measured, as shown in Figure 6. To establish an evaluation, the stress signal and cumulative damage resulting from a classical fixed-speed startup are also included in the analysis. Subsequently, the cumulative damage associated with the three distinct startup trajectories is normalized with the cumulative damage derived from the classical fixed-speed startup. In Figure 6, the measured and predicted stress-time signals for each start-up sequences A), B) and C) are compared to the stress-time signal resulting from the classical fixed-speed startup. Notably, the maximum amplitude of these stress signals reaches approximately 1.8 times the operating setpoint at the Best Efficiency Point (BEP), as observed during a standard fixed-speed startup.

The first observation reveals a similarity in the damage distribution (di) between the 2-slopes and linear start-up methods. These similarities come from average stress amplitudes ranging between 0.8 and 1.2 times the BEP value. These stress fluctuations are the primary contributors to this observed damage distribution pattern. In contrast, both BEP tracking and classical fixed-speed start-ups show a comparable trend, characterized by cumulative damage influenced by low-cycle fatigue. This type of damage occurs within stress ranges of 1.5 to 1.7 times the BEP value, which has a low number of cycles.

Regarding signal prediction, the predicted stress signal provides a reliable estimate of the cumulative damage, with discrepancies of less than one order of magnitude of all startup trajectories. Furthermore, the damage distribution patterns (di) between the predicted stress signals and the actual measurements show similarities. Nonetheless, it's important to note that there exist certain variations between the predicted stress signals and the observed measurements. The prediction accuracy in the same order of magnitude for the different start-ups D_{pred}/D_{meas} are, respectively for the 2-slopes start-up $D_{pred}/D_{meas}=1.97$, for the BEP tracking start-up $D_{pred}/D_{meas}=2.83$ and for the linear start-up

 D_{pred}/D_{meas} =0.69. It notice that some patterns based on a Δt =2s are repeated on the predicted stress signals. These patterns are induced by the sampling time at the construction of the Voronoi cells, which has been set to Δt =2s for this test case. It's interesting to compare the different trajectories and observe the relative variations between them and not necessarily look at the absolute value of the damage, which is strongly linked to the hypothesis of fatigue calculations. It can be mentioned that for the BEP tracking startup, the cumulative damage is much lower than for all the other startups, especially compared to the classical fixed-speed start-up.

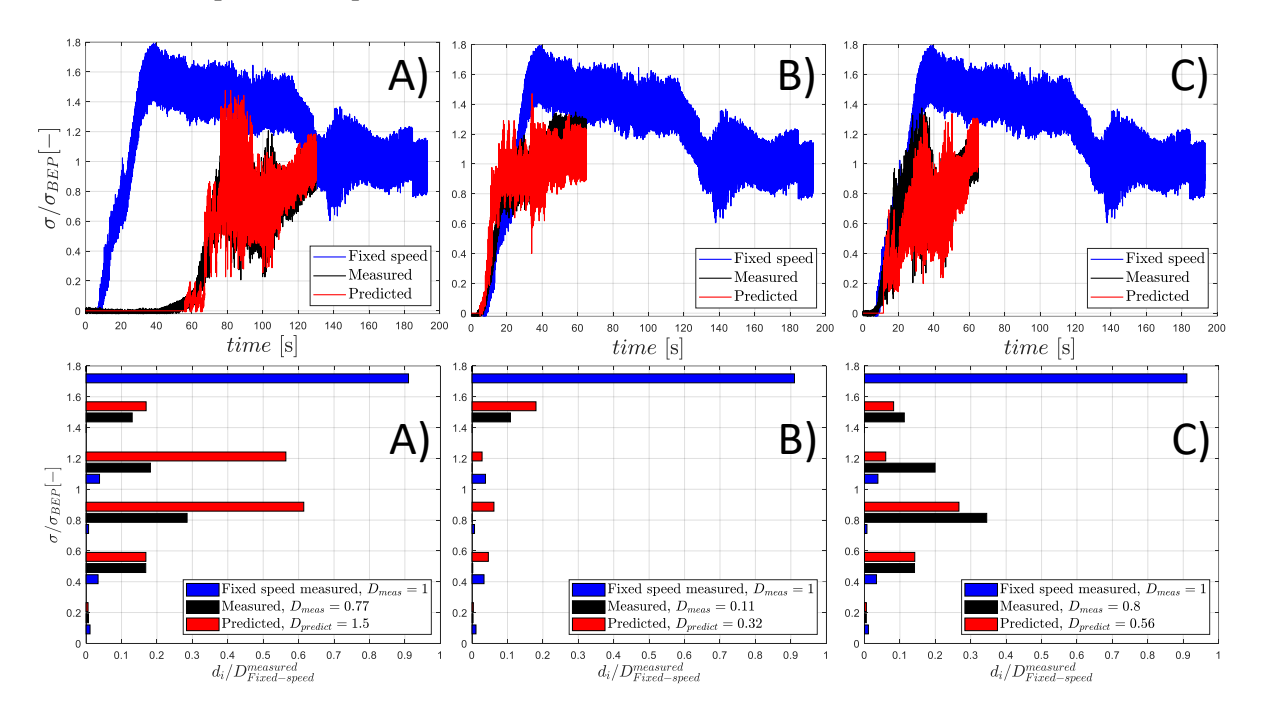


Figure 6:The measured and predicted stress signals are represented for the three start-up including the measured classical fixed-speed start-up. The absolute damage and damage distribution results of the reconstructed signals (red) are compared with those of the measured signals (black) for the three different predictions: A) 2-slopes start-up, B) BEP tracking start-up and C) linear start-up trajectory. The cumulated damage is compared and normalized with the classical fixed-speed start-up (blue).

5. Conclusion

The method presented for estimating the cumulative damage of a start-up sequence using time stress signal on the turbine runner blades has been applied for comparison with measurements on a similar reduced scale model of the Z'Mutt Francis pump-turbine. These experimental measurements include onboard strain gauges on the runner, which are used to construct a Voronoi diagram of transient stress signals using discretized start-up transient signals and to predict runner damage during a new start-up trajectory. This transient mapping method predicts cumulative runner damage by recombining the entire time stress signal of a start-up sequence, taking into account the mean value of the stress. The time signal predictions are relatively accurate and the average stress value is close enough to calculate the cumulative damage for a given sequence. Cumulative damage based on reconstruction gives the same order of magnitude as damage based on measurement. However, deviations between measurement and prediction are still present, with a deviation of a factor of 2 for 2-slope startup, 2.8 for BEP and 0.7 for linear. More generally, all variable-speed start-up reduce runner damage compared to the classical fixedspeed start-up. The runner damage generated by the BEP tracking start-up is around 9 times smaller than the classical one. This method can therefore be used to find an optimized trajectory for a pump-turbine start-up sequence. In order to refine the Voronoi mapping and obtain even more accurate results, transient data from start-ups could be combined and overlaid with stationary data from the different operating points.

6. Acknowledgements

The Hydropower Extending Power System Flexibility (XFLEX HYDRO) project has received funding from the European Union's Horizon 2020 research and innovation programme under grant agreement No 857832. The authors would like to thank CKD Blansko, Hydro Exploitation SA and Alpiq SA for their collaboration and support.

References

- [1] https://xflexhydro.net/
- [2] S Alligné, et al., Turbine mode start-up simulation of a FSFC variable speed pump-turbine prototype Part I:1D simulation, Proceedings of IAHR 2020, Lausanne, Switzerland.
- [3] J Löfflad, M Eissner, Lifetime assessment and plant operation optimization based on geometry scan and strain gauge testing START/STOP optimization, 10th International conference on hydraulic efficiency measurements, Itajuba, Brazil, 2014.
- [4] V Hasmatuchi, et al., Detection of harsh operating conditions on a Francis prototype based on insitu non-intrusive measurements, Proceedings of Hydro 2019, Porto, Portugal.
- [5] M Gagnon, J Nicolle, On variations in turbine runner dynamic behaviours observed within a given facility, 2019 IOP Conf. Ser.: Earth Environ. Sci. 405 012005
- [6] D Biner, et al., Numerical fatigue damage analysis of a variable speed Francis pump-turbine during start-up in generating mode, Proceedings of IAHR 2022, Trondheim, Norway
- [7] M Seydoux, et al., Assessments of hydropower plants start-up sequences and equivalent runner damage under transient operation, Proceedings of IAHR 2022, Trondhein, Norway
- [8] J Schmid, et al., Optimization of turbine start-up sequence of a full size frequency converter variable speed pump-turbine, Proceedings of IAHR 2022, Trondhein, Norway
- [9] M Gagnon, et al., The role of high cycle fatigue (HCF) onset in Francis runner reliability, 2012 IOP Conf. Ser.: Earth Environ. Sci. 15 022005
- [10] ASTM E1049-85(2017) West Conshohocken. Standard Practices for Cycle Counting in Fatigue Analysis, 2011.
- [11] F. Kun, H. A. Carmona, J. S. Andrade, and H. J. Herrmann. Universality behind Basquin's Law of Fatigue. Physical Review Letters, 100(9):094301, March 2008.
- [12] Wilhelm Weber, Carsten Mende, and Jiri Koutnik, Advanced fatigue analysis for transient operating conditions of Francis turbines, 2014 IOP Conf. Ser.: Earth Environ. Sci. 22 032054
- [13] Q Du, et al., Centroidal Voronoi Tessellations: Applications and Algorithms, 1999, Society for Industrial and Applied Mathematics, Vol. 41, No. 4, pp. 637–676.
- [14] Sonsino et al., Korrosionsschwingfestigkeit der Stahlgusssorten G-X5CrNi13 4 und G-X5CrNi17 4 für Laufräder von Wasserkraftmaschinen und Pumpen, Werkstoffe und Korrosion, (1990), 41,330-342.